We are IntechOpen, the world's leading publisher of Open Access books
Built by scientists, for scientists

4,800
Open access books available

122,000
International authors and editors

135M
Downloads

Our authors are among the

154
Countries delivered to

TOP 1%
most cited scientists

12.2%
Contributors from top 500 universities

CLARIVATE ANALYTICS
BOOK CITATION INDEX
INDEXED

WEB OF SCIENCE™

Selection of our books indexed in the Book Citation Index in Web of Science™ Core Collection (BKCI)

Interested in publishing with us?
Contact book.department@intechopen.com

Numbers displayed above are based on latest data collected.
For more information visit www.intechopen.com

Chapter

A Simple Way to Produce Gold Nanoshells for Cancer Therapy

Rosa Isela Ruvalcaba Ontiveros, José Alberto Duarte Moller, Anel Rocío Carrasco Hernandez, Hilda Esperanza Esparza-Ponce, Erasmo Orrantia Borunda, Cynthia Deisy Gómez Esparza and Juan Manuel Olivares Ramírez

Abstract

Gold nanoshells (GNSs), formed by a silica core surrounded by a gold shell, present a shift on their surface plasmon resonance (SPR) to the near-infrared (NIR) part of the electromagnetic spectrum when synthesized with specific dimensions. This chapter presents a simple method to prepare the nanoshells, a step-by-step characterization, as well as their absorbance spectrum. For the synthesis, silica spheres, with approximately 190 ± 5 nm in diameter, were prepared using the Stöber method and then functionalized with 3-aminopropyltriethoxysilane (APTES). The gold nanoparticles (GNPs), with a diameter of 7 ± 3 nm, were produced by the reduction of chloroauric acid. Then, the silica was seeded with the GNPs to later grow a gold shell with the help of $Au(OH)_4^-$ ions and formaldehyde. UV-Vis spectroscopy results showed an increase of absorbance starting at 520 nm. It reached its maximum around 600 nm and kept absorbing all through 1200 nm. Transmission electron microscope (TEM) and scanning electron microscope (SEM) images suggest that the absorption peak movement coincided with the completion of the shell. Furthermore, when the sample was irradiated with an 820 nm wavelength/3.1 mW laser, its temperatures increased by 6.3°C in 2 min, showing its absorbance in the NIR.

Keywords: gold, nanoshells, surface plasmon resonance, near-infrared absorption, silica core, core-shell particles

1. Introduction

There are hundreds of types of cancer, and each one has different characteristics [1]. Therefore, science utilizes the most innovative discoveries in an effort to find new treatments, and nanotechnology offers a wide variety of options. One example of this is the nanoparticle colloids. They can be designed to concentrate on specific organs (passive targeting), or their surfaces can be modified by an antibody or ligand to get attached to a specific target (active targeting) [2]. Furthermore, metallic nanoparticles, like GNS, present interesting optical properties. The shell, formed by GNPs, confines the plasmons to the surface of the particle, changing the plasmon frequency of the gold. Therefore, the GNSs absorb different wavelengths than gold

in bulk. Moreover, when the wavelength of the incident light is larger than the size of the nanoparticle exciting the plasmons at their natural resonance frequency, light is absorbed more strongly causing an increase in temperature. When the GNSs are synthesized with specific geometry and dimensions, their SPR changes causing their absorption to shift to the NIR region of the electromagnetic spectrum [3]. This shift offers a great potential for applications in the medical field because GNPs are bio-inert [4], and the cytotoxicity of the silica has been widely studied [5]. Additionally, the wavelengths of the NIR spectrum are considered the optical window of the human body. As a result, while most biological soft tissues have low absorption of these wavelengths [6], GNSs absorb them causing them to increase their temperature.

GNSs have been synthesized over different templates. Polystyrene cores claim to offer a narrower plasmon resonance absorption peak due to their higher reflective index [7]; iron oxide nanoparticles present a superparamagnetic template useful for magnetic resonance imaging [8]; silver nanoparticles have also been used as a mold for hollow gold nanoshells [9]. However, the functionalization of the polystyrene takes more time, reactants, and supervision which increases the chances of error as compared with the functionalization of the silica. Besides, the cytotoxicity of the silica nanoparticles makes them a good option for medical applications. Moreover, once the GNS is produced, the silica core can be diluted with hydrochloric acid to obtain hollow gold nanoparticles [10] that can be used for the controlled release of drugs [11] due to their capacity for encapsulating sensitive materials and their low thermal expansion coefficient. Therefore, providing a simpler and more efficient method of synthesis of GNS on silica templates provides a more promising variety of applications like for photothermal therapy [12], optical imaging [13], and drug release [2], as well as providing a near instantaneous in situ whole blood assay [14].

The synthesis of the GNSs has been extensively explored. Different methods, like reflux systems [15] or flow micro-reactors [16], can be used as well as procedures involving high temperatures [17]. But most of those methods last over 30 h [18]. In this chapter, we present a simple and effective method of preparation that shortens the time of the traditional procedures published before and uses only a magnetic stirrer with heating for the synthesis.

The reductions of the time were obtained by first modifying the Stöber method of synthesis of silica particles from 2 h to 30 min Samples were obtained at 30, 60, 90, and 120 min throughout the reaction to determine the minimum time of reaction needed. Also, the seeding process can be shortened from 2 h to 30 min. During the seeding process, where the silica is decorated with GNPs, a sample was obtained using only 30 min of resting time and compared with another sample obtained after the full 2 h of the resting time previously suggested. In both cases, SEM images were obtained showing that 30 min were sufficient to accomplish the synthesis of the silica as well as their seeding. In consequence, the total time of the process was reduced by 3 h.

2. Background

The "Birth of Nanotechnology" was the title used by David Thompson [19] on his article acknowledging Michael Faraday's synthesis of gold nanoparticles in 1857. What Faraday called "Colloidal Ruby Gold" [20] was, in fact, a solution of dispersed GNPs so small that no microscope of that time was able to observe them. It wasn't until 1985 that Turkevich et al. [21] used an electron microscope to corroborate that Faraday's ruby gold was formed by GNPs with an average size of 6 ± 2 nm. Separately, in 1967 Werner Stöber et al. developed a method of synthesizing silica spheres in the micron size range [22] to be used especially in the medical field due to its known cytotoxicity, and in 1998 they were used by Naomi Halas et al. as the templates of GNS [23].

3. Experimental

3.1 Materials

Ethanol (100%), tetraethyl orthosilicate (TEOS) (98%), 3-aminopropyl-triethoxysilane (APTES) (99%), trisodium citrate dihydrate, gold (III) chloride trihydrate ($HAuCl_4$, 49%), formaldehyde (37%), and sodium borohydride ($NaBH_4$, 98%) were purchased from Sigma-Aldrich. Potassium carbonate (K_2CO_3, 99%) and ammonium hydroxide (28%) were purchased from J.T. Baker. All the solutions were prepared with deionized water.

3.2 Characterization

Images were obtained using the field-emission scanning electron microscope (SEM, JEOL JSM-7401F) and the transmission electron microscope (TEM, HT7700 Hitachi). For the ultraviolet-visible (UV-Vis) spectra, the Evolution 220 spectrophotometer UV-Vis (Thermo Scientific) was used. The FTIR spectra were obtained with an IRAffinity-1S Fourier transform infrared spectrophotometer (Shimadzu). The sample was irradiated with an 820 nm wavelength/3.1 mW laser (Multi-Channel Fiber-Coupled Laser Source, Thorlabs), and the infrared images were taken with a Non-contact Digital IR Thermometer (TrueIR Agilent Keysight U5855A). Measurement of the particles and histograms were acquired with the Image J® software [24].

3.3 Preparation of silica spheres

Silica particles were prepared by modifying the Stöber method [22]. About 50 ml of ethanol, 2.5 ml of deionized water, and 4.25 ml of ammonium hydroxide were magnetically stirred in an 80 ml glass flask for 5 min. Then, 0.75 ml of TEOS was added dropwise. The solution was heated at 40°C. Temperature and agitation were kept for 2 h. The color of the solution changed from transparent to opaque white approximately 10 min after adding the TEOS as shown in **Figure 1**. This time corresponds to the induction period needed to form the SiO_2 nucleus from the concentration used of the TEOS monomer [25]. Samples were obtained at 30, 60, 90, and 120 min after adding the TEOS to observe the evolution of the process.

3.4 Functionalization of the silica spheres

In order to create open links over the silica to attach the GNPs, the silica was functionalized with APTES on a 1 ml:1 μl silica/APTES volume ratio. About 50 ml

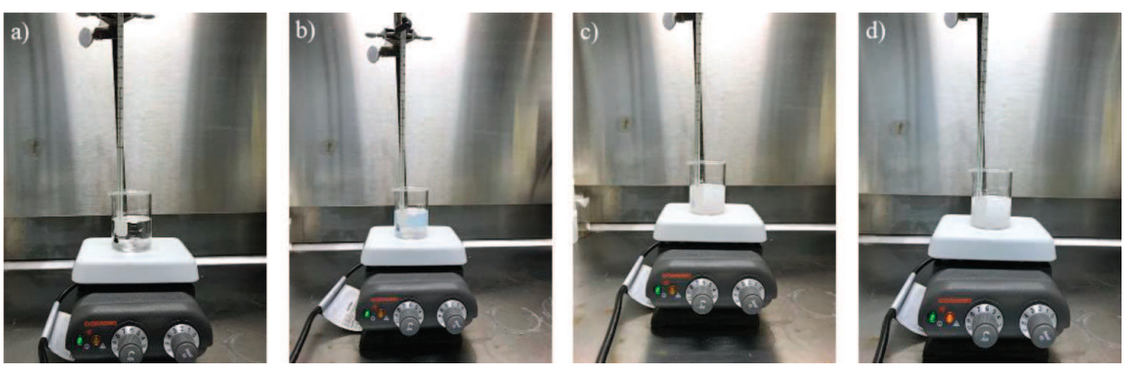

Figure 1.
Images of the synthesis of SiO_2 particles: (a) right after adding TEOS, (b) at 10 min of reaction, (c) at 30 min of reaction, and (d) at 2 h of reaction.

of the silica template solution was magnetically stirred for 5 min with 50 μl of APTES in an 80 ml glass flask. The solution was left still overnight at room temperature. The opaque white functionalized silica particles precipitated in the solution leaving a clear fluid at the top. To separate the functionalized silica, the mixture was centrifuged at 6000 rpm for 1.5 min and washed in deionized water three times. Finally, they were sonicated in 20 ml of deionized water final volume.

3.5 Synthesis of gold nanoparticles

The method presented by Abdollahi et al. [10] was followed to elaborate the GNPs. First, 100 ml of deionized water at room temperature was placed in a 140 ml flask under magnetic agitation. Then 1 ml of 1% $HAuCl_4$ solution, 2 ml of 1% trisodium citrate, and 1 ml of freshly made 0.075% $NaBH_4$ in 1% trisodium citrate were added in that order. The mixture was stirred for 10 min and used immediately to avoid the agglomeration. The GNP may also be stored at 4°C in an amber glass bottle for later use.

Throughout the synthesis, the gold solution changed its color from light yellow (**Figure 2a**) to wine red (**Figure 2b**). This is a characteristic of the GNP formation [26].

3.6 Seeding process

For the seeding process, 100 ml of GNPs and 10 ml of functionalized silica were magnetically stirred in a 140 ml glass flask for 5 min as shown in **Figure 3a**. Then, it was left still for 2 h. **Figure 3b** presents how the seeded silica spheres precipitated and changed their color from opaque white to lavender, while the mother solution changed from wine red to transparent. The mixture was centrifuged at 6000 rpm for 2 min and washed in deionized water three times. Finally, it was sonicated in 20 ml of deionized water final volume. The same procedure was followed, but the solution was left still for only 30 min to observe the development of the seeding process through time.

3.7 Gold hydroxide solution

For the shell growth process, a gold hydroxide solution was prepared by mixing 100 ml of 2 mM K_2CO_3 solution and 1.5 ml of 1% $HAuCl_4$ in a 140 ml glass flask for

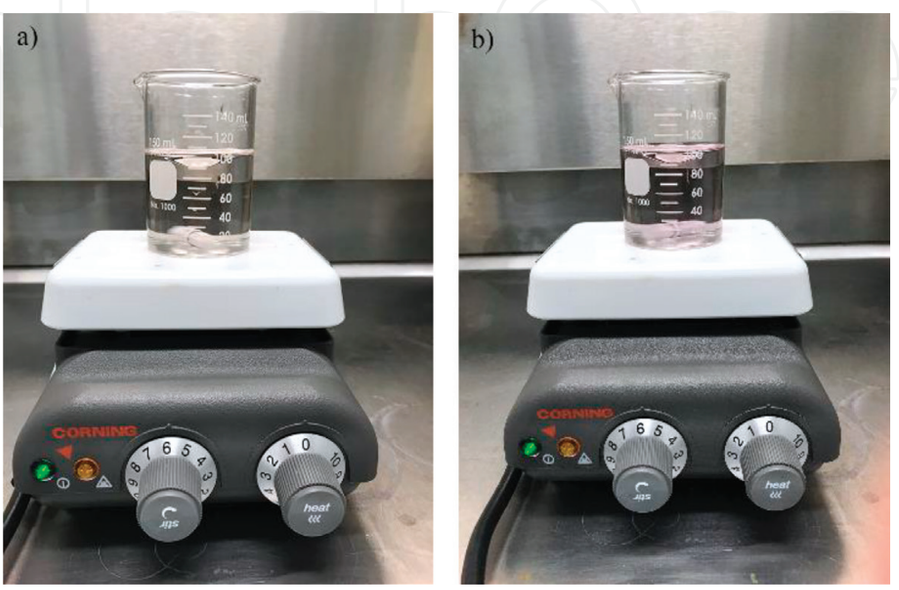

Figure 2.
Synthesis of GNPs at (a) the beginning of the reaction and (b) after 10 min of reaction.

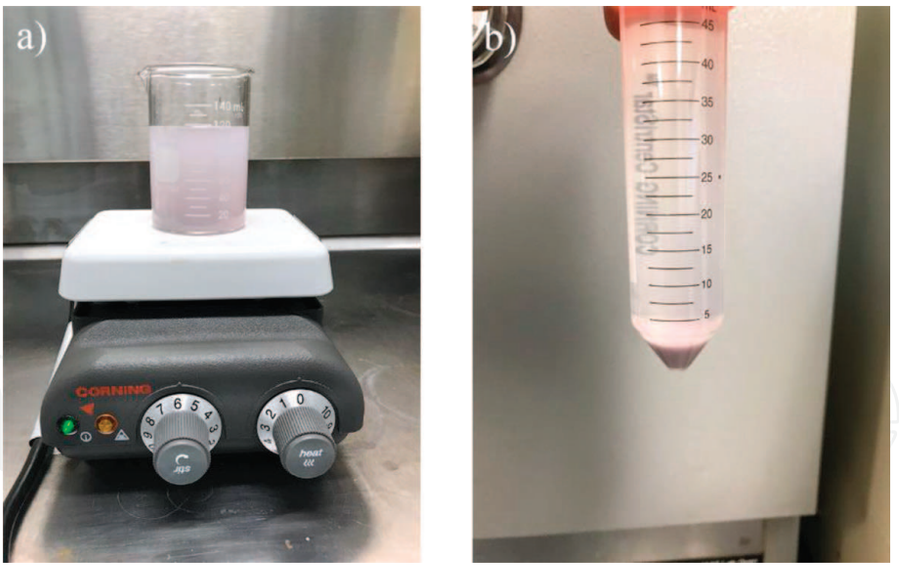

Figure 3.
Images at (a) the beginning of the seeding process and (b) after 2 h of resting time.

30 min. The color of the solution changed from light yellow (**Figure 4a**) to transparent (**Figure 4b**). It was left still overnight at room temperature in an amber glass bottle to facilitate the formation of $Au(OH)_4^-$ ions [18].

3.8 Shell growth

The shell was developed from the gold seeds deposited over the functionalized silica particles with the help of the $Au(OH)_4^-$ ions. About 100 ml of the gold hydroxide solution (**Figure 5a**) and 5 ml of seeded silica were magnetically stirred in a 140 ml glass flask for 5 min (**Figure 5b**). Next, 5 ml of formaldehyde was added to the solution (**Figure 5c**) and stirred for 10 min (**Figure 5d**). The solution was left still for 50 min. Finally, it was centrifuged at 6000 rpm for 2 min, washed, and dispersed in 10 ml of deionized water final volume.

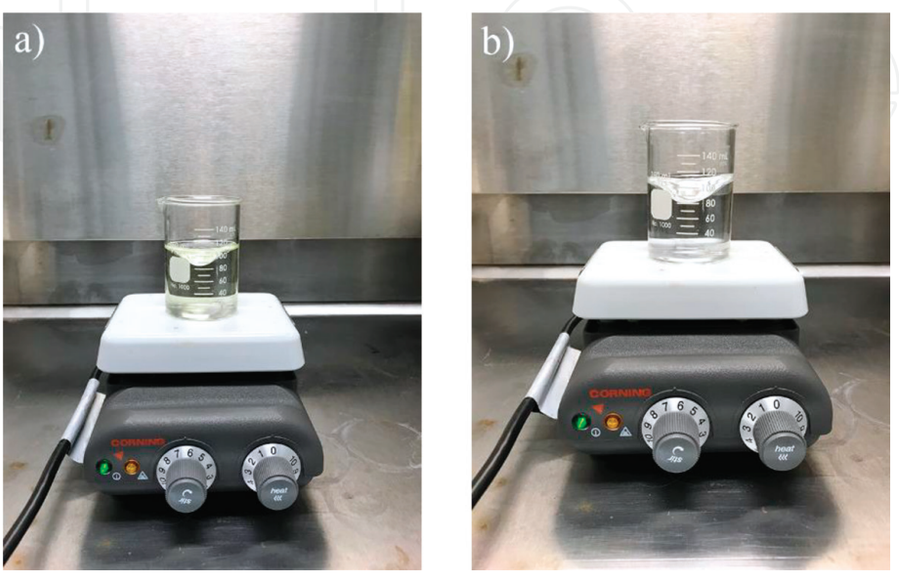

Figure 4.
Images illustrating the change of color of the gold hydroxide solution at (a) the beginning of the synthesis (light yellow) and (b) 30 min of reaction (transparent).

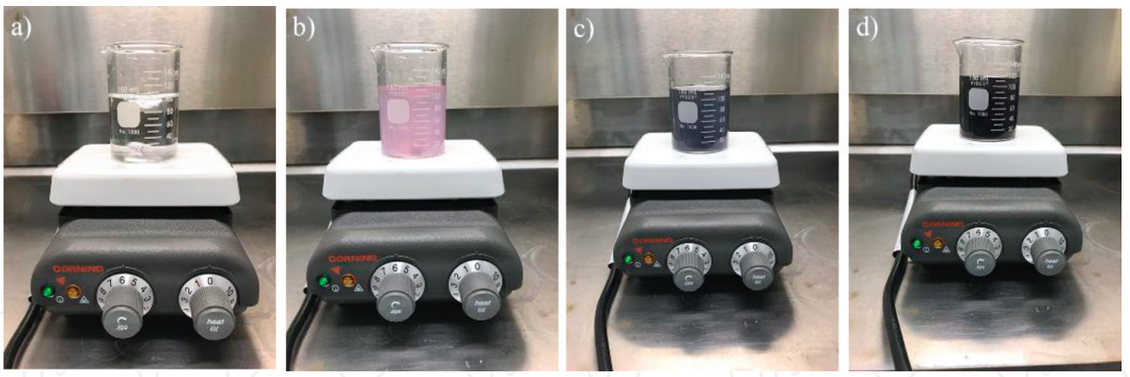

Figure 5.
Images of the shell growing process. (a) Gold hydroxide solution, (b) gold hydroxide + seeded silica, (c) gold hydroxide + seeded silica + formaldehyde, and (d) solution after 10 min of reaction.

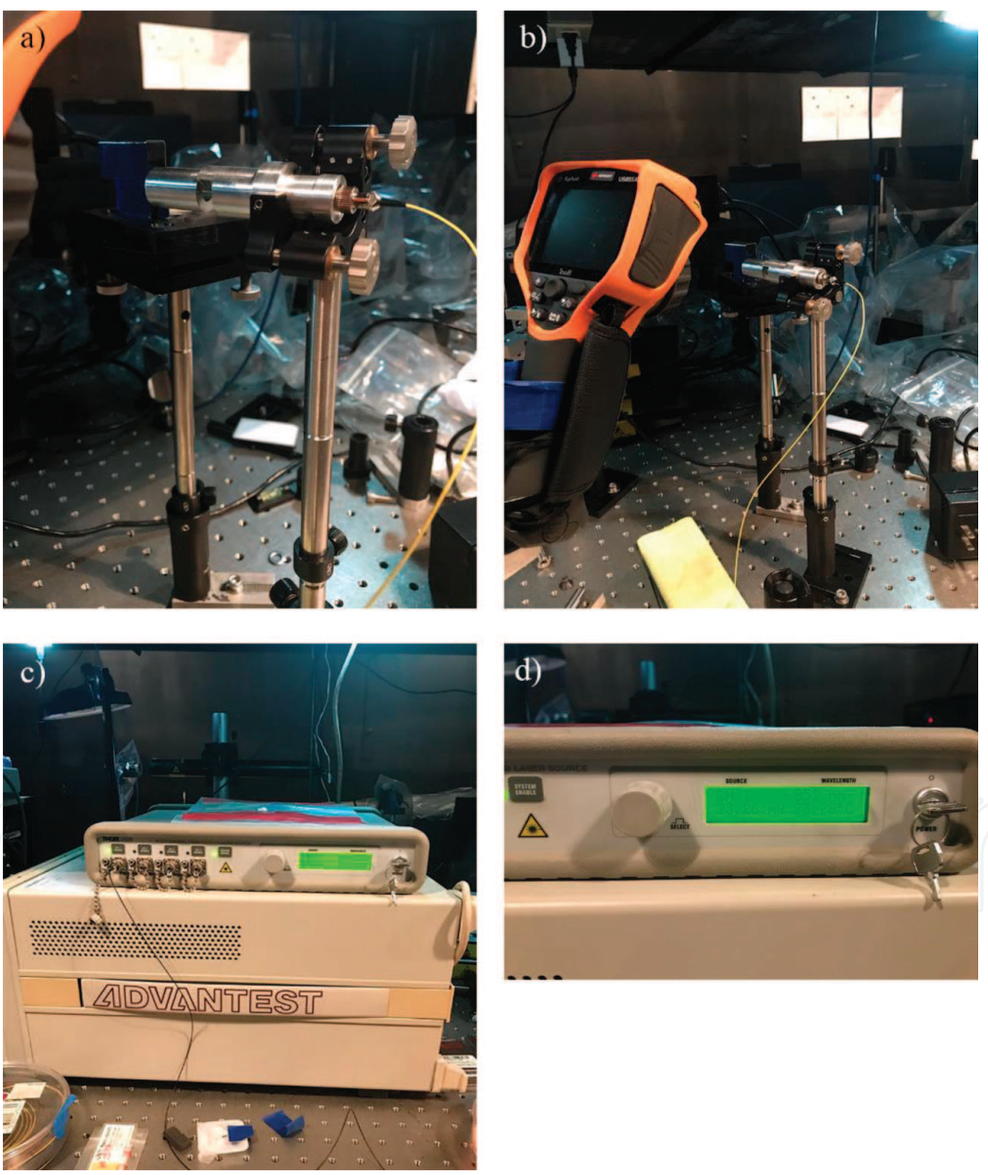

Figure 6.
Images of the installation of the (a) 820 nm wavelength laser, (b) non-contact digital IR thermometer, (c) connection to the multi-channel laser source, and (d) selection of the channel with the desired wavelength.

3.9 Thermography

To obtain the IR images, first, the 820 nm wavelength laser was fastened to the support for it to aim directly to the sample (**Figure 6a**). Then the Digital IR

thermometer was also secured and directed to the GNS (**Figure 6b**). Next, the laser was connected to the Multi-channel laser source (**Figure 6c**). Finally, the channel with the desired wavelength was selected (**Figure 6d**), and the irradiation was started.

4. Results and discussion

4.1 Characterization of the silica templates

TEM images obtained from the silica samples taken at 30, 60, 90, and 120 min after adding the TEOS are presented in **Figure 7**. When comparing the images, no significant variation in the size of the silica particles is noticeable.

To corroborate that the silica particles do not change substantially when the reaction time is over 30 min, the images were studied with the software Image J®, and the diameter distribution of the particles was analyzed. Over 1000 particles from the different samples were measured to obtain the histograms presented in **Figure 8** where samples A, B, C, and D correspond to 30, 60, 90, and 120 min of reaction time, respectively. They illustrate that the diameter distribution of the silica spheres throughout the synthesis oscillates around the 190 ± 5 nm on all the samples.

To have a better understanding of the information, **Table 1** contains useful statistic information from the samples.

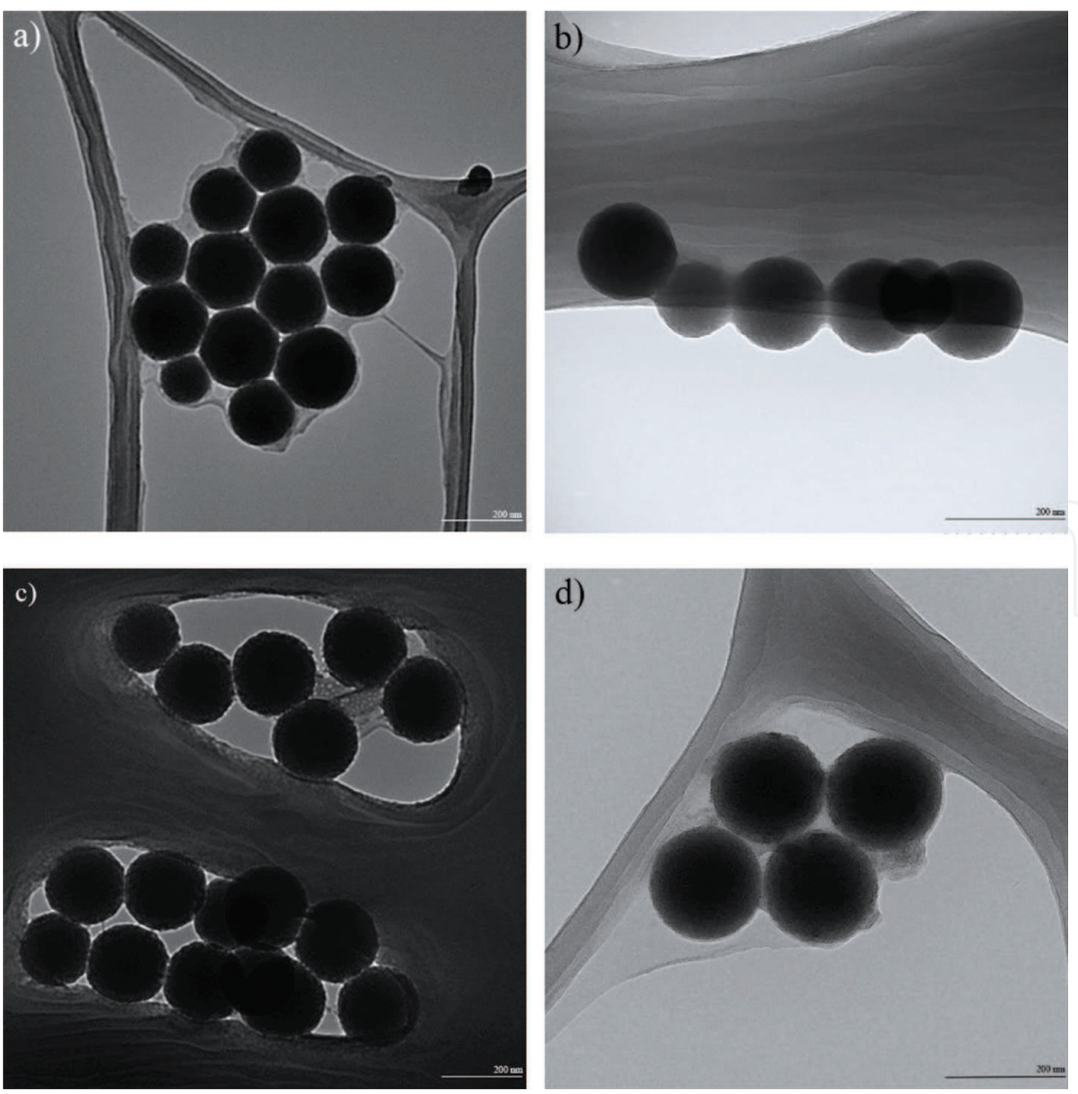

Figure 7.
TEM images of silica particles at (a) 30, (b) 60, (c) 90, and (d) 120 min after adding TEOS.

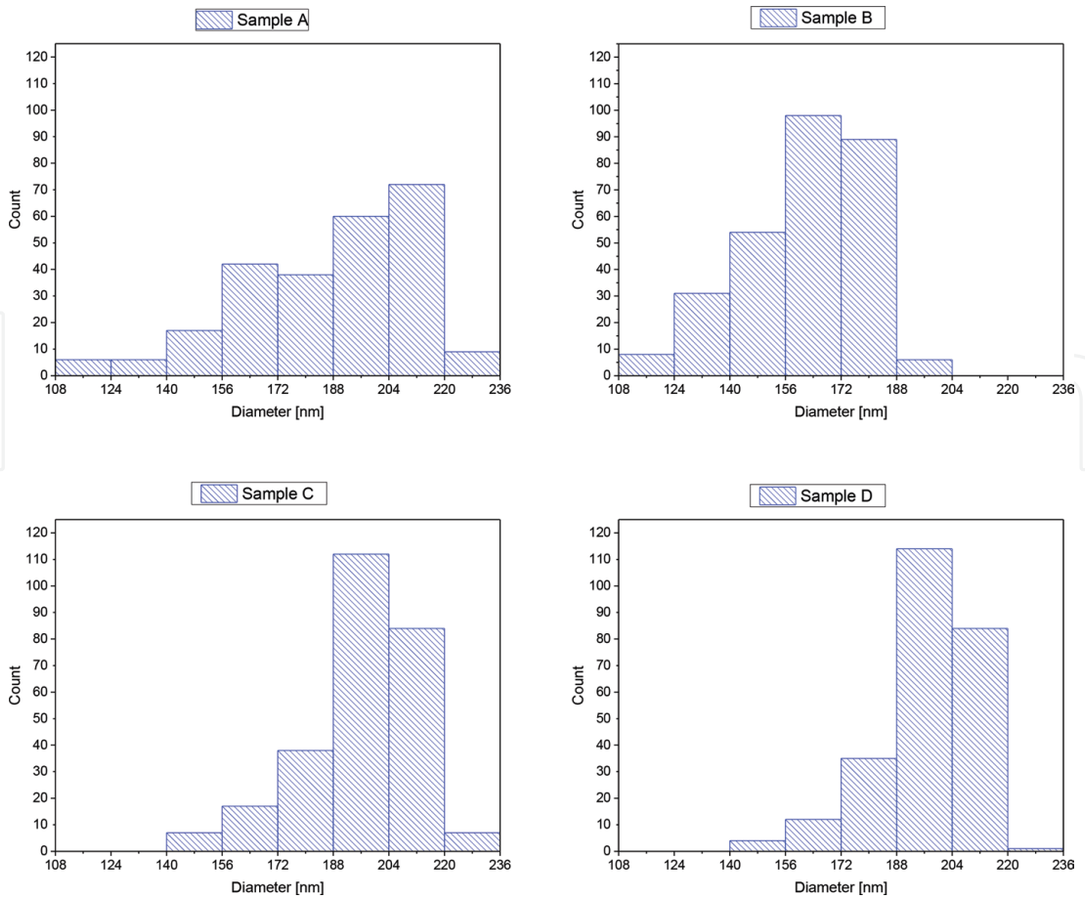

Figure 8.
Histograms illustrating the diameter distribution of the silica particles throughout their synthesis.

	Count	Mean	Std dev.	Mode
Sample A	250	187	25	197 (79)
Sample B	287	162	18	162 (80)
Sample C	265	196	16	201 (92)
Sample D	250	197	13	198 (105)

Table 1.
Statistic information obtained by measuring the diameters of silica particles from the different samples.

The mean, standard deviation, and mode obtained after analyzing the samples show that, in general, the silica templates keep their size and shape after 30 min of synthesis. Therefore, the objective of synthesizing silica particles with diameters of 190 ± 5 nm was achieved within 30 min of reaction time. More than 30 min of synthesis does not result in any relevant change in the sample. For this reason, the total process time can be reduced from 2 h to 30 min, shortening the reaction time by 1 h and 30 min when compared with similar published works where the synthesis time is at least 2 h [10, 17, 27, 28].

4.2 Characterization of the functionalized silica templates

The functionalization of the silica with a primary amine group ($–NH_2$) was accomplished by the use of APTES which changed the superficial charge of the

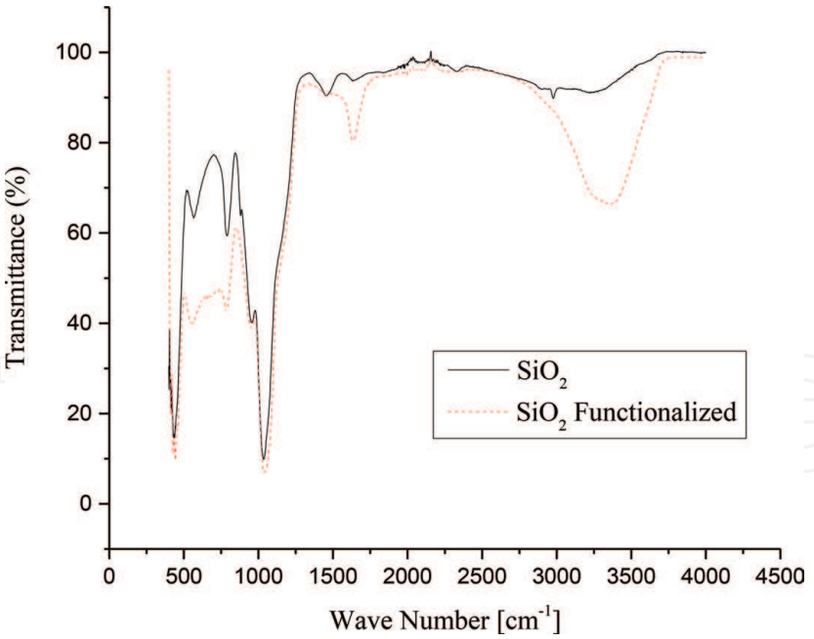

Figure 9.
FTIR spectrum of silica particles and silica particles functionalized with APTES.

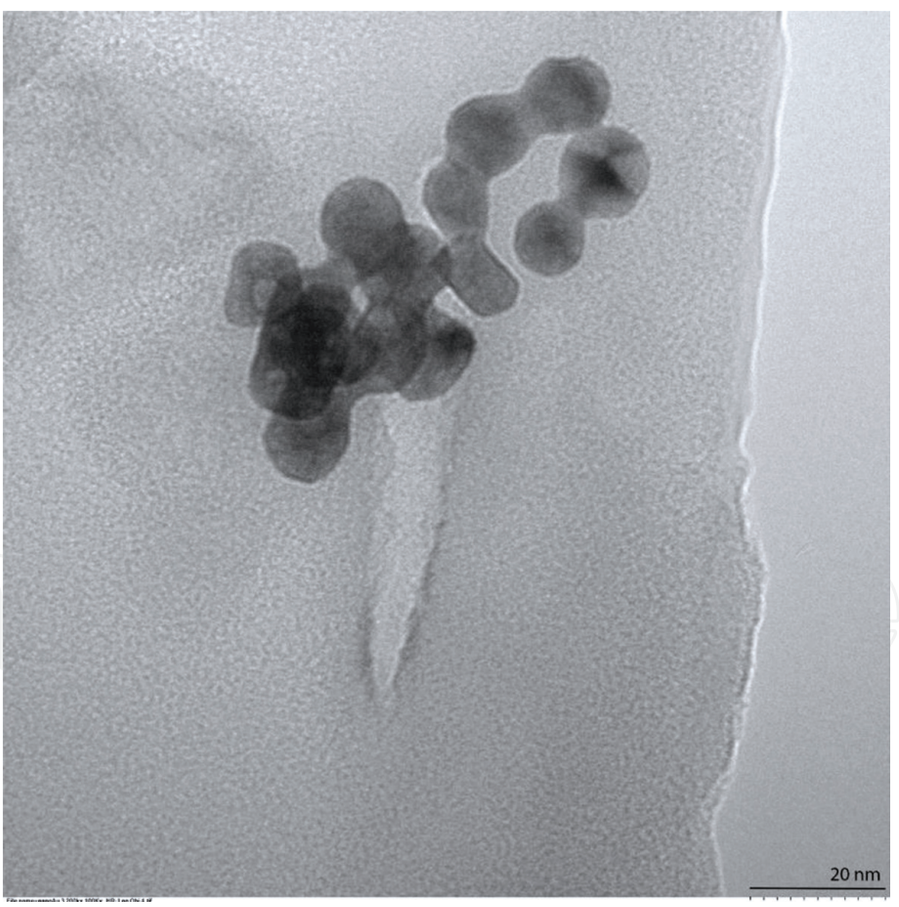

Figure 10.
TEM images of GNPs.

silica providing an electrostatic link for the GNPs to attach [29]. This superficial modification was verified by the FTIR spectrum shown in **Figure 9** where the vibrations of primary amines are found between 3550 and 3330 cm^{-1} which correspond to the vibrations of a primary amine group [30].

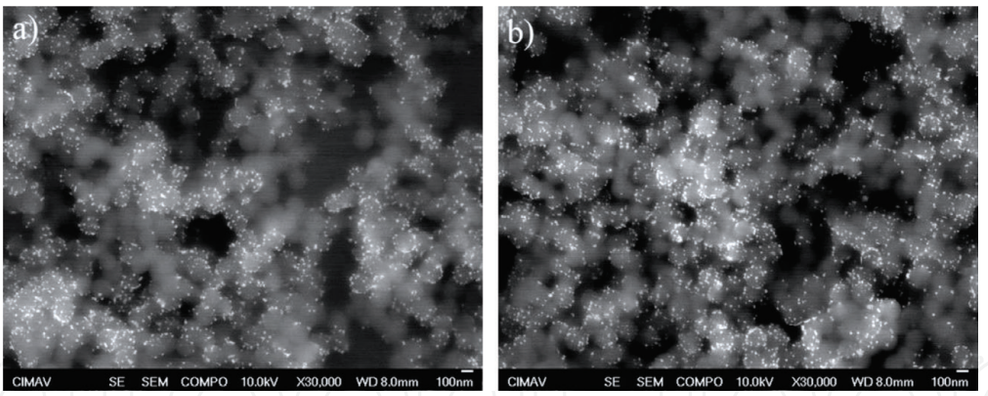

Figure 11.
SEM images illustrating the seeding process with (a) 30 min of resting time and (b) 2 h of resting time.

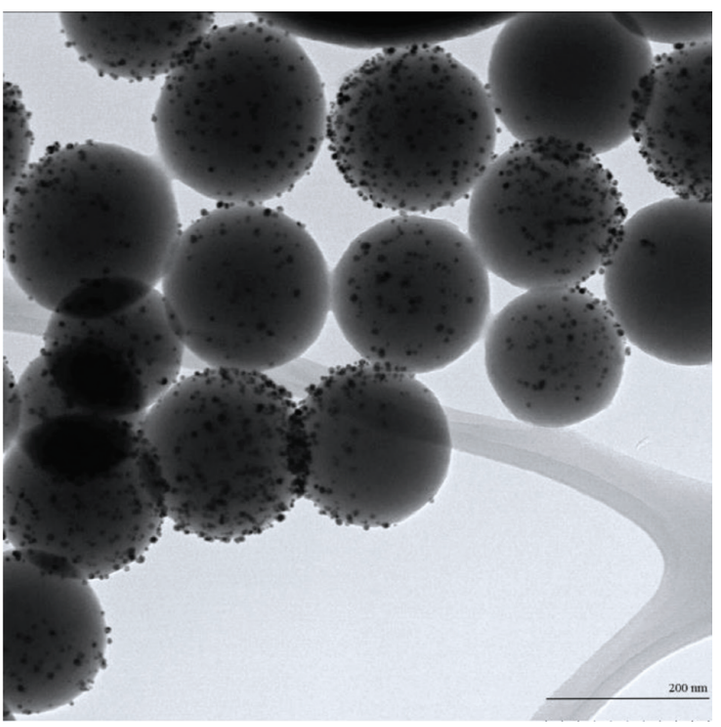

Figure 12.
TEM image of a gold decorated silica particle.

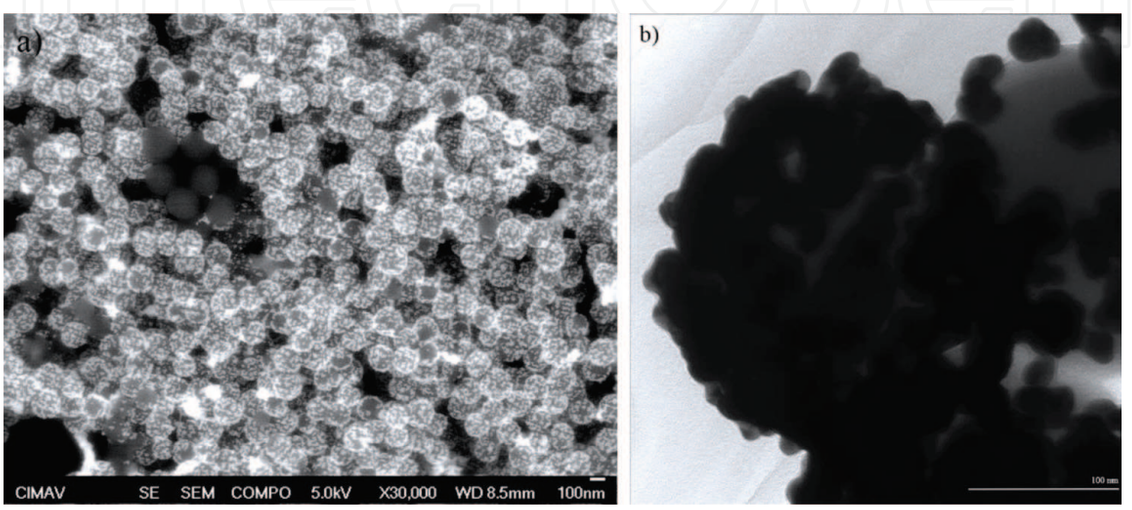

Figure 13.
(a) SEM and (b) TEM images of GNS.

4.3 Characterization of the gold nanoparticles and seeded silica

The GNPs were analyzed under a TEM. **Figure 10** illustrates the GNPs with a diameter of 7 ± 3 nm and spherical shape overall.

The seeding process was followed with 2 h of still time as well as with 30 min of still time. The first and second samples were observed under the microscope. The samples were taken with the purpose of observing the development of the seeds. **Figure 11a** presents an SEM image of seeded silica with 30 min of resting time, while **Figure 11b** presents an SEM image of seeded silica with 2 h of resting time. The images show that 30 min is enough time to create the seeds because both images display approximately the same number of nucleus per silica particle.

Even though a complete shell was not formed, the seeds are ready to grow the gold shell on the next step. A TEM image of a seeded silica particle is presented in **Figure 12**. This image corroborates the seeding process as well as the silica functionalization.

4.4 Characterization of the gold nanoshells

Figure 13a and **b** presents SEM and TEM images of the synthesized GNS, respectably. They illustrate that the silica particles are almost surrounded by gold. The higher density of gold, the separation of the GNPs [31], and the dielectric properties of the silica [3] contribute to the absorption of the NIR wavelength, which causes the increase in temperature.

4.5 The UV-Vis spectrum

Figure 14 presents the UV-Vis spectrum of the particles through the process. Silica particles, as well as functionalized silica particles, do not show significant

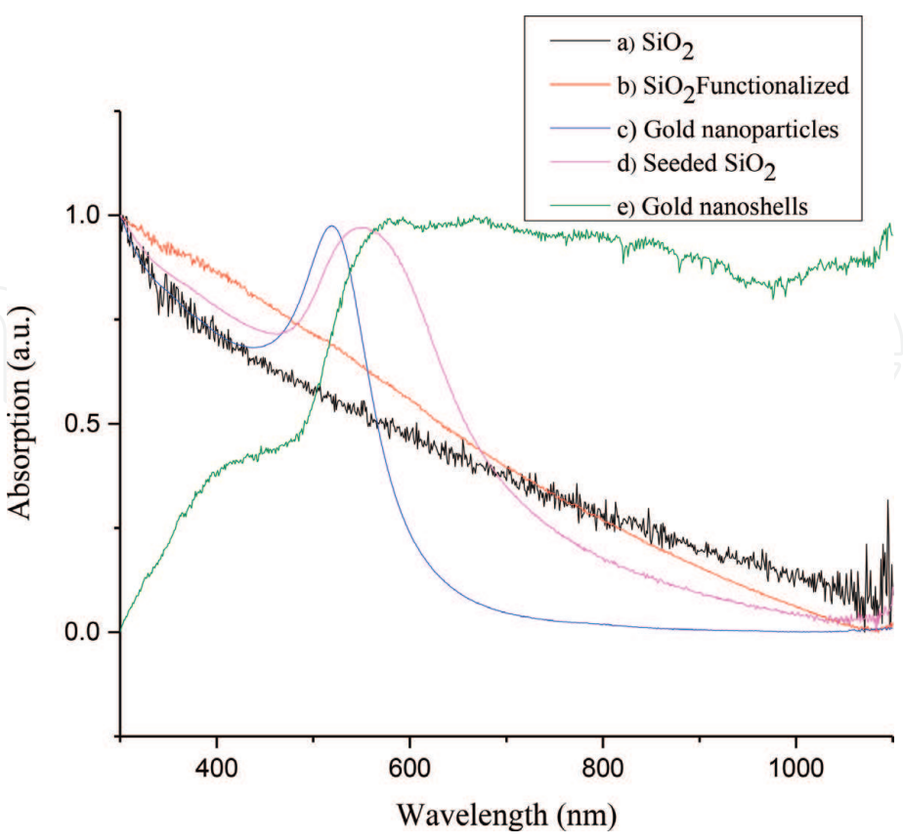

Figure 14.
UV-Vis spectrum of (a) silica, (b) functionalized silica, (c) gold nanoparticles, (d) gold seeded silica, and (e) gold nanoshells.

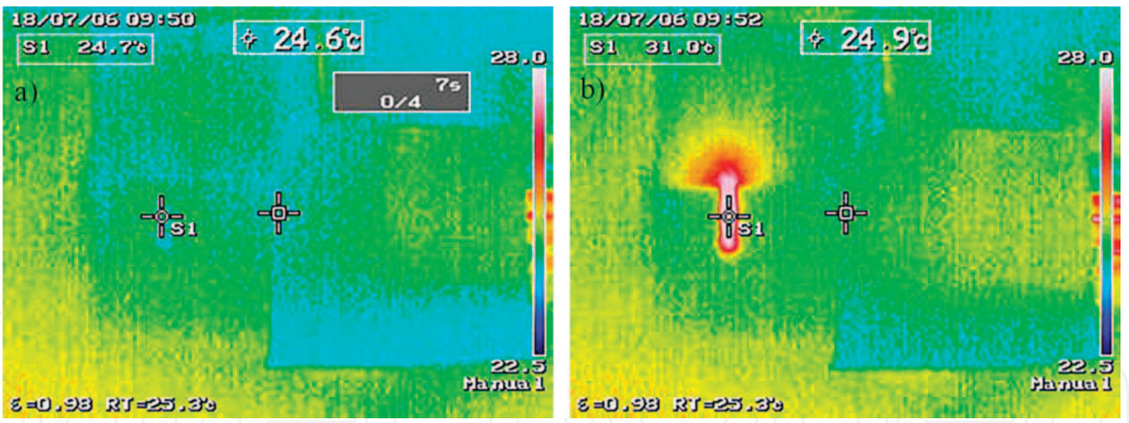

Figure 15.
Thermography images of the GNS taken (a) before and (b) after being irradiated with 840 nm wavelength laser for 2 min.

absorption on the NIR. As for the GNPs, they exhibit their characteristic absorption between 520 and 530 nm [29]. However, on the seeded silica particles, the slight shift to the NIR is noticeable. While on the GNS, the peak not only shifted to the NIR, but it kept a high absorbance all the way to 1100 nm. This range is part of the optical window of the human body [5]. The absorbance of the GNSs is due to the SPR that creates an electric field on the surface increasing the absorption of these wavelengths. SPR happens when metal nanoparticles are irradiated with a wavelength bigger than their size, exciting the electrons of the conducting band [2].

4.6 Heat generation of GNS from light energy

To verify the absorbance of the GNS, they were irradiated with an 840 nm laser with a power of 3.1 mW. **Figure 15a** and **b** displays the thermography images of the sample while being irradiated at time zero and 2 min later. The temperature of the sample increased from 24.7 to 31.0°C. This confirms that GNSs are able to absorb light from the NIR and convert it in heat.

5. Conclusions

Synthesizing GNS by seeding and growing a gold shell over silica spheres with GNPs showed to be an effective method to tune their absorption to the NIR. The SEM and TEM images show the evolution of the process, while the absorbance spectrum displays the GNS shifting over the NIR. Therefore, we obtained a simple technique of producing GNS that can be used for medical applications thanks to the bio-inert GNPs [3] and the widely studied cytotoxicity of the silica [5]. This method does not require long periods of time, when compared with previously published mechanisms, and does not need sophisticated equipment.

Acknowledgements

We thank Consejo Nacional de Ciencia y Tecnologia (Conacyt) and Centro de Investigacion en Materiales Avanzados (CIMAV) for the financial support, Dr. Jose Guadalupe Murillo Ramirez for his help with the use of 852 nm wavelength laser, Dr. Pedro Piza for lending us the thermographic camera, Ing. Wilber Antunez Flores, and M.C. Karla Campos Venegas for helping us obtain the TEM and SEM images.

Nomenclature

GNSs	gold nanoshells
SPR	surface plasmon resonance
NIR	near-infrared
APTES	3-aminopropyltriethoxysilane
GNP	gold nanoparticles
TEM	transmission electron microscope
SEM	scanning electron microscope
TEOS	tetraethyl orthosilicate

Author details

Rosa Isela Ruvalcaba Ontiveros[1], José Alberto Duarte Moller[1*], Anel Rocío Carrasco Hernandez[1], Hilda Esperanza Esparza-Ponce[1], Erasmo Orrantia Borunda[1], Cynthia Deisy Gómez Esparza[1] and Juan Manuel Olivares Ramírez[2]

1 Centro de Investigación en Materiales Avanzados (CIMAV), Chihuahua, México

2 Universidad Tecnológica de San Juan del Río, San Juan del Río, México

*Address all correspondence to: alberto.duarte@cimav.edu.mx

IntechOpen

© 2019 The Author(s). Licensee IntechOpen. This chapter is distributed under the terms of the Creative Commons Attribution License (http://creativecommons.org/licenses/by/3.0), which permits unrestricted use, distribution, and reproduction in any medium, provided the original work is properly cited. CC BY

References

[1] Instituto Nacional del Cáncer. Tipos de Cancer [Internet]. 2015. Available from: https://www.cancer.gov/espanol/tipos

[2] Pissuwan D, Valenzuela SM, Cortie MB. Therapeutic possibilities of plasmonically heated gold nanoparticles. Trends in Biotechnology. 2006;**24**(2):62-67. DOI: 10.1016/j.tibtech.2005.12.004

[3] Petryayeva E, Krull UJ. Localized surface plasmon resonance: Nanostructures, bioassays and biosensing—A review. Analytica Chimica Acta. 2011;**706**(1):8-24. Available from: http://linkinghub.elsevier.com/retrieve/pii/S0003267011011196

[4] Jenkins JT, Halaney DL, Sokolov KV, Ma LL, Shipley HJ, Mahajan S, et al. Excretion and toxicity of gold-iron nanoparticles. Nanomedicine: Nanotechnology, Biology and Medicine. 2013;**9**(3):356-365. DOI: 10.1016/j.nano.2012.08.007

[5] Spyrogianni A, Sotiriou GA, Brambilla D, Leroux J-C, Pratsinis SE. The effect of settling on cytotoxicity evaluation of SiO_2 nanoparticles. Journal of Aerosol Science. 2017;**108**(January):56-66. Available from: https://linkinghub.elsevier.com/retrieve/pii/S0021850216302166

[6] Anderson RR, Parrish JA. The optics of human skin. The Journal of Investigative Dermatology. 1981;**77**(1):13-19. DOI: 10.1111/1523-1747.ep12479191

[7] Yong K-T, Sahoo Y, Swihart MT, Prasad PN. Synthesis and plasmonic properties of silver and gold nanoshells on polystyrene cores of different size and of gold-silver core-shell nanostructures. Colloids and Surfaces A: Physicochemical and Engineering Aspects. 2006;**290**(1-3):89-105. Available from: http://linkinghub.elsevier.com/retrieve/pii/S0927775706003542

[8] Mohammad F, Al-Lohedan HA. Luteinizing hormone-releasing hormone targeted superparamagnetic gold nanoshells for a combination therapy of hyperthermia and controlled drug delivery. Materials Science and Engineering: C. 2017;**76**:692-700. DOI: 10.1016/j.msec.2017.03.162

[9] Sun Y, Xia Y. Increased sensitivity of surface plasmon resonance of gold nanoshells compared to that of gold solid colloids in response to environmental changes. Analytical Chemistry. 2002;**74**(20):5297-5305. DOI: 10.1021/ac0258352

[10] Abdollahi SN, Naderi M, Amoabediny G. Synthesis and characterization of hollow gold nanoparticles using silica spheres as templates. Colloids and Surfaces A: Physicochemical and Engineering Aspects. 2013;**436**:1069-1075. DOI: 10.1016/j.colsurfa.2013.08.028

[11] David Lou XW, Archer LA, Yang Z. Hollow micro-/nanostructures: Synthesis and applications. Advanced Materials. 2008;**20**(21):3987-4019. DOI: 10.1002/adma.200800854

[12] Wang L, Yuan Y, Lin S, Huang J, Dai J, Jiang Q, et al. Photothermo-chemotherapy of cancer employing drug leakage-free gold nanoshells. Biomaterials. 2016;**78**:40-49. DOI: 10.1016/j.biomaterials.2015.11.024

[13] Tuersun P, Han X. Optimal design of gold nanoshells for optical imaging and photothermal therapy. Optik. 2014;**125**(14):3702-3706. DOI: 10.1016/j.ijleo.2014.03.007

[14] Hirsch LR, Jackson JB, Lee A, Halas NJ, West JL. A whole blood immunoassay using gold nanoshells. Analytical Chemistry. 2003;**75**(10):2377-2381. DOI: 10.1021/ac0262210

[15] Brito-Silva AM, Sobral-Filho RG, Barbosa-Silva R, de Araújo CB, Galembeck A, Brolo AG. Improved synthesis of gold and silver nanoshells. Langmuir. 2013;**29**(13):4366-4372. DOI: 10.1021/la3050626

[16] Watanabe S, Asahi Y, Omura H, Mae K, Miyahara MT. Flow microreactor synthesis of gold nanoshells and patchy particles. Advanced Powder Technology. 2016;**27**(6):2335-2341. DOI: 10.1016/j.apt.2016.08.013

[17] Phonthammachai N, Kah JCY, Jun G, Sheppard CJR, Olivo MC, Mhaisalkar SG, et al. Synthesis of contiguous silica-gold core-shell structures: Critical parameters and processes. Langmuir. 2008;**24**(9):5109-5112. DOI: 10.1021/la703580r

[18] Abdollahi SN, Naderi M, Amoabediny G. Synthesis and physicochemical characterization of tunable silica-gold nanoshells via seed growth method. Colloids and Surfaces A: Physicochemical and Engineering Aspects. 2012;**414**:345-351. DOI: 10.1016/j.colsurfa.2012.08.043

[19] Thompson D. Michael Faraday's recognition of ruby gold: The birth of modern nanotechnology. Gold Bulletin. 2007;**40**(4):267-269. DOI: 10.1007/BF03215598

[20] Faraday M. The Bakerian lecture: Experimental relations of gold (and other metals) to light. Philosophical Transactions. Royal Society of London. 1857;**147**:145-181. DOI: 10.1098/rstl.1857.0011

[21] Turkevich J. Colloidal gold. Part II. Gold Bulletin. 1985;**18**(4):125-131. DOI: 10.1007/BF03214694

[22] Stöber W, Fink A, Bohn E. Controlled growth of monodisperse silica spheres in the micron size range. Journal of Colloid and Interface Science. 1968;**26**(1):62-69. Available from: http://linkinghub.elsevier.com/retrieve/pii/0021979768902725

[23] Westcott SL, Oldenburg SJ, Lee TR, Halas NJ. Formation and adsorption of clusters of gold nanoparticles onto functionalized silica nanoparticle surfaces. Langmuir. 1998;**14**(19):5396-5401. DOI: 10.1021/la980380q

[24] ImageJ [Internet]. 2018. Avaliable from: https://imagej.nih.gov/ij/

[25] Pham T, Jackson JB, Halas NJ, Lee TR. Preparation and characterization of gold nanoshells coated with self-assembled monolayers. Langmuir. 2002;**18**(12):4915-4920. DOI: 10.1021/la015561y

[26] Pandey PC, Pandey G, Walcarius A. 3-Aminopropyltrimethoxysilane mediated solvent induced synthesis of gold nanoparticles for biomedical applications. Materials Science and Engineering: C. 2017;**79**:45-54. DOI: 10.1016/j.msec.2017.05.009

[27] Lee SH, Jamison AC, Hoffman DM, Jacobson AJ, Lee TR. Preparation and characterization of polymeric thin films containing gold nanoshells via electrostatic layer-by-layer self-assembly. Thin Solid Films. 2014;**558**:200-207. DOI: 10.1016/j.tsf.2014.02.021

[28] Elbialy N, Mohamed N, Monem AS. Synthesis, characterization and application of gold nanoshells using mesoporous silica core. Microporous and Mesoporous Materials. 2014;**190**:197-207. DOI: 10.1016/j.micromeso.2014.02.003

[29] Wei X, Liu Z, Jin X, Huang L, Gurav DD, Sun X, et al. Plasmonic nanoshells enhanced laser desorption/ionization

mass spectrometry for detection of serum metabolites. Analytica Chimica Acta. 2017;**950**:147-155. DOI: 10.1016/j.aca.2016.11.017

[30] Socrates G. Infrared and Raman characteristic group frequencies. 3rd ed. West, Sussex: John Wiley & Sons. Journal of Raman Spectroscopy. 2004;**35**:905-905. DOI: 10.1002/jrs.1238

[31] Huang X, El-Sayed MA. Gold nanoparticles: Optical properties and implementations in cancer diagnosis and photothermal therapy. Journal of Advanced Research. 2010;**1**(1):13-28. Available from: http://linkinghub.elsevier.com/retrieve/pii/S2090123210000056

IntechOpen